


## Comment on “Effect of liquid temperature on sonoluminescence”

Yuri A. Pishchalnikov

*Burst Laboratories, Inc., 13346A Grass Valley Ave., Grass Valley, California 95945, USA*

 (Received 29 March 2017; revised manuscript received 10 December 2017; published 5 February 2018)

It has been suggested that bubble-wall velocities cannot exceed the sound speed in the liquid at the bubble wall [K. Yasui, *Phys. Rev. E* **64**, 016310 (2001)]. Here we show that this upper bound was derived omitting the partial derivatives with respect to time, i.e., assuming that the flow was in the steady state. For collapsing bubbles, however, the steady-flow assumption requires justification, as the partial time derivatives appear to have the same orders of magnitude as the other terms in Euler’s and the continuity equations. Furthermore, numerical solutions of the hydrodynamic equations with a HYADES hydrocode yielded supersonic velocities in the liquid at and near the collapsing bubble. We also show the spatial distributions of pressure, density, sound speed, and mass flux density around the supersonically collapsing bubble.

DOI: [10.1103/PhysRevE.97.027101](https://doi.org/10.1103/PhysRevE.97.027101)

High bubble-wall velocities have been predicted since works of Besant [1] and Rayleigh [2], showing an infinite growth of the bubble-wall velocity during the implosion of an empty spherical cavity in incompressible liquids [3]. The sound speed in incompressible liquids is infinite, and the flow velocities are subsonic. In compressible liquids, the sound speed is finite, and the flow can be supersonic. In the supersonic flow, sound waves propagate only downstream [3]. Hence, for a supersonically imploding bubble, no sound can leave the supersonic shell around the bubble, and the bubble behaves like a black hole for sound. The upstream flow becomes independent of pressure and density variations downstream and in the bubble.

Intriguingly, it has been suggested that the fundamental theory of fluid dynamics imposes an upper bound on the bubble-wall velocity so that it cannot exceed the sound speed in the liquid at the bubble wall [4]. If valid, this upper bound would have significant consequences, limiting collapse velocities and, as a consequence, the extreme conditions produced by the collapsing bubbles. This is particularly important for applications involving violent implosions of bubbles, such as in attempts to achieve thermonuclear fusion [5–9], or for intense cavitation at high static pressures [5,10–27]. So far, however, the upper bound has been considered in only a few numerical studies [4,28]. Moreover, the upper bound disagrees with previous investigations predicting bubble-wall velocities greater than the speed of sound [29–31]. To help resolving this disagreement, we discuss the assumptions made in deriving the upper bound in Ref. [4].

There are examples when the theory of fluid dynamics imposes a sonic limit on fluid velocity [3]. For one, it is impossible to achieve supersonic velocities with a steady flow in a continually narrowing tube, a converging nozzle [3]. This result may appear, at first, to support the validity of the upper bound, as the spherically symmetric flow around the bubble can conceivably be subdivided into flows through a plurality of frictionless tubes converging at the bubble center. However, as later discussed, the flow in the converging tube was assumed to be invariable with time, i.e., in the steady state [3].

Here we show that the steady-flow assumption was also used to derive the upper bound in Ref. [4]. For the collapsing bubbles, however, the fluid velocity, density, and pressure vary with time [1–3], so the applicability of the steady-flow assumption requires justification. We show that the partial time derivatives have the same orders of magnitude as the other terms in hydrodynamic equations. This raises a question on the validity of omitting the partial time derivatives in deriving the upper bound in Ref. [4]. We also show results of a numerical simulation with a HYADES hydrocode [32], yielding bubble-wall velocities faster than sound. Finally, we discuss the mass flux density for subsonic and supersonic steady flows, and show the mass flux density for the unsteady flow around the imploding bubble.

The upper bound was derived from Euler’s equation

$$\frac{\partial \mathbf{u}}{\partial t} + (\mathbf{u} \cdot \mathbf{grad}) \mathbf{u} = -\frac{1}{\rho} \mathbf{grad} P \quad (1)$$

and the equation of continuity

$$\frac{\partial \rho}{\partial t} + \text{div}(\rho \mathbf{u}) = 0, \quad (2)$$

where  $\mathbf{u}$  is the fluid velocity,  $t$  is time,  $\rho$  is the density, and  $P$  is the pressure [3].

For a radially symmetric flow, spatially dependent only on the distance  $r$  from the center of the bubble, Eqs. (1) and (2) can be written as follows [3]:

$$\frac{\partial u}{\partial t} + u \frac{\partial u}{\partial r} = -\frac{1}{\rho} \frac{\partial P}{\partial r}, \quad (3)$$

$$\frac{\partial \rho}{\partial t} + \frac{1}{r^2} \frac{\partial (\rho u r^2)}{\partial r} = 0. \quad (4)$$

For a steady flow, the partial time derivatives vanish:

$$u \frac{\partial u}{\partial r} = -\frac{1}{\rho} \frac{\partial P}{\partial r}, \quad (5)$$

$$\frac{1}{r^2} \frac{\partial (\rho u r^2)}{\partial r} = 0. \quad (6)$$

Equations (5) and (6) lead to the equations used to derive the upper bound in Ref. [4], specifically, Eq. (A1)

$$u \, du = - \frac{dP}{\rho} = - \frac{dP}{d\rho} \frac{d\rho}{\rho} = - c^2 \frac{d\rho}{\rho} \quad (7)$$

and Eq. (A3)

$$\frac{d\rho}{\rho} + \frac{du}{u} + \frac{dA}{A} = 0, \quad (8)$$

where  $c$  is the sound speed and  $A$  is the cross section of the fluid flow perpendicular to the flow direction [4].

Thus, the upper bound in Ref. [4] appears to be derived omitting the partial time derivatives  $\partial u/\partial t$  and  $\partial \rho/\partial t$ . To justify this steady-flow assumption, one needs to show that the partial time derivatives are negligible in comparison with the other terms in Euler's and the continuity equations. In Euler's equation, the ratio of the convective term  $u \, \partial u/\partial r$  to the partial time derivative  $\partial u/\partial t$  is on the order of

$$\frac{u \, \frac{\partial u}{\partial r}}{\frac{\partial u}{\partial t}} \sim \frac{u \, \frac{\Delta u}{\Delta r}}{\frac{\Delta u}{\Delta t}} \sim \frac{u}{\frac{\Delta r}{\Delta t}}, \quad (9)$$

where  $\Delta t$  is a time and  $\Delta r$  is a length on the order of the times and distances over which the fluid velocity undergoes significant changes  $\Delta u$  [3]. For example, for a sinusoidal sound,  $\Delta r$  is on the order of a wavelength and  $\Delta t$  is on the order of a period, so the ratio  $\Delta r/\Delta t$  is on the order of the sound speed  $c$ , and the ratio (9) is on the order of  $u/c$ . The velocity  $u$  is often smaller than  $c$ , and the convective term  $u \, \partial u/\partial r$  is smaller than  $\partial u/\partial t$ .

For the bubble wall, the ratio  $\Delta r/\Delta t$  is on the order of the bubble-wall velocity  $U$ . The liquid velocity  $u$  at the bubble wall is also  $U$ . Hence, the ratio (9) is on the order of one, suggesting that the partial time derivative  $\partial u/\partial t$  has the same order of magnitude as the convective term  $u \, \partial u/\partial r$ .

Likewise, in the continuity equation, the ratio of the term  $u \, \partial \rho/\partial r$  to the partial time derivative  $\partial \rho/\partial t$  is on the order of

$$\frac{u \, \frac{\partial \rho}{\partial r}}{\frac{\partial \rho}{\partial t}} \sim \frac{u \, \frac{\Delta \rho}{\Delta r}}{\frac{\Delta \rho}{\Delta t}} \sim \frac{u}{\frac{\Delta r}{\Delta t}}, \quad (10)$$

and, at the bubble wall, is on the order of one. This suggests that the partial time derivative  $\partial \rho/\partial t$  is on the same order of magnitude as the term  $u \, \partial \rho/\partial r$ .

If one neglects both of these terms as being small in comparison with the other terms in the continuity equation, the upper bound is meaningless. Indeed, the sum of these two terms is the material time derivative  $d\rho/dt$ , which describes the density variations at the bubble wall as it moves in space. Neglecting  $d\rho/dt$  leads to the incompressible approximation with an infinite sound speed, making the upper bound meaningless.

This assessment is supported by numerical simulations showing supersonic liquid velocities at and in the proximity to the collapsing bubbles [29–31]. We modeled a spherically symmetric bubble using the one-dimensional (1D) HYADES code (Cascade Applied Sciences, Inc., USA). HYADES is a Lagrangian hydrodynamics and energy transport code, originally

developed to model dense plasma [32] and later adapted for modeling cavitation bubbles [5,10–15].

We modeled a 50- $\mu\text{m}$  argon bubble in water. Initially, water and gas were in thermal equilibrium at temperature  $T$  of 297 K and at rest. The outer boundary of water, located at 101.6 mm from the bubble, was driven by an oscillatory pressure  $P(t) = P_0 - P_a \sin(2\pi f t)$  [33]. The driving frequency  $f$  was 25982 Hz, corresponding to one of the spherically symmetric resonance modes of the fluid volume [5,10–27]. The static pressure  $P_0$  was 20 MPa; the acoustic pressure  $P_a$  at the outer boundary of water was 2 MPa. This pressure wave spherically converged to the center, producing a net negative pressure that expanded the bubble to the radius  $R_{\text{max}} \approx 0.83$  mm with the growth-collapse cycle lasting  $\sim 14.5 \, \mu\text{s}$  [26].

For modeling, the bubble and the liquid were divided into concentric zones. We used 16–64 zones in the bubble and 1000–1500 zones in the liquid, decreasing zone sizes for finer resolution near the collapse [5,10–15,26]. Zones moved with the mass. HYADES does not model mass diffusion, and the amount of gas in the bubble remained unchanged. HYADES also does not include a number of other liquid-gas interface phenomena, such as vaporization, condensation, dissociation, and surface tension. The Laplace pressure produced by the surface tension, however, appeared to be insignificant for the bubble sizes and pressure modeled here. Specifically, the Laplace pressure for the smallest bubble radius [ $R_{\text{min}} \approx 23 \, \mu\text{m}$  at the moment of the collapse, Fig. 1(a)] was less or about 0.01 MPa, i.e., smaller than the static pressure by three orders of magnitude.

Apparently, the 1D code does not model any surface instabilities at the liquid-gas interface. As a consequence, the spherical model of the bubble diverged from the experimental observations showing a microjet and daughter microbubbles during the rebound [26]. We modeled only the first growth-collapse cycle of the bubble. The pressure, density, and temperature during the collapse are shown in Ref. [26] (Fig. 2 and video 1); here we show primarily the liquid velocity and the sound speed.

HYADES calculates the sound speed using equations of state and the relation

$$c^2 = \left( \frac{\partial P}{\partial \rho} \right)_S = \left( \frac{\partial P}{\partial \rho} \right)_T + \left( \frac{\partial P}{\partial T} \right)_\rho \left( \frac{\partial T}{\partial \rho} \right)_S, \quad (11)$$

where  $S$  is the entropy. The thermodynamic derivatives  $(\partial P/\partial \rho)_T$  and  $(\partial P/\partial T)_\rho$  are found directly from the equations of state. The derivative  $(\partial T/\partial \rho)_S$  is found using a Maxwell's relation

$$\left( \frac{\partial T}{\partial \rho} \right)_S = \frac{1}{\rho^2} \left( \frac{\partial P}{\partial S} \right)_\rho \quad (12)$$

and the equation

$$\left( \frac{\partial P}{\partial S} \right)_\rho = T \left( \frac{\partial P}{\partial E} \right)_\rho, \quad (13)$$

which follows from the second law of thermodynamics  $dE = T dS - P dV$ , where  $E$  is the internal energy and  $V$  is the volume. Inserting (12) and (13) in Eq. (11) gives

$$c^2 = \left( \frac{\partial P}{\partial \rho} \right)_T + \frac{\alpha T}{\rho^2} \left( \frac{\partial P}{\partial T} \right)_\rho, \quad (14)$$

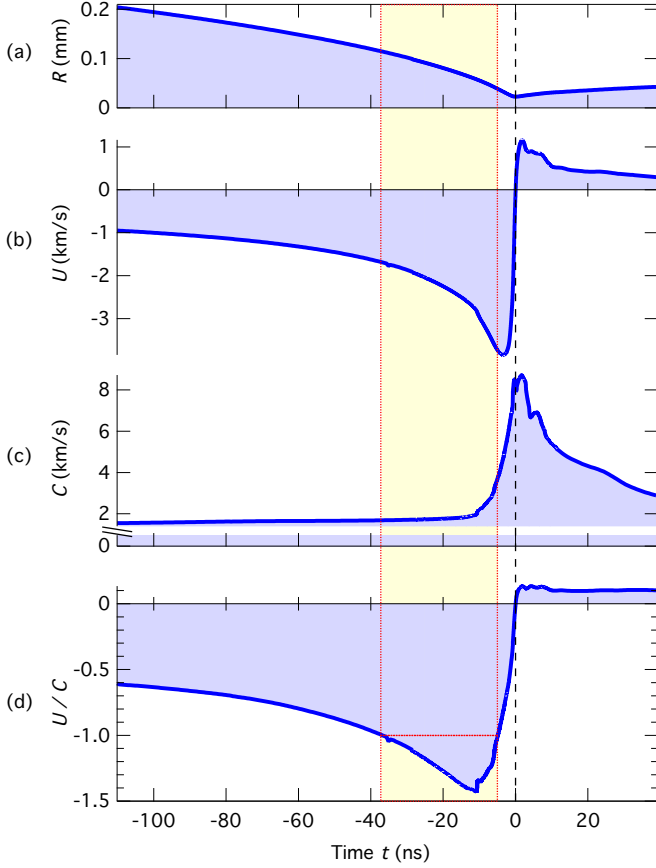


FIG. 1. Bubble radius  $R(t)$ , bubble-wall velocity  $U(t)$ , sound speed in the liquid at the bubble wall  $C(t)$ , and the bubble-wall Mach number  $U/C$ . The bubble-wall velocity  $U(t)$  was negative during the implosion phase ( $t < 0$ ) until the moment of the collapse (dashed line). A dotted-line rectangle highlights the time interval ( $-36.7$  to  $-4.9$  ns) when the bubble-wall velocity was supersonic ( $|U| > C$ ).

where  $\alpha = (\partial P/\partial T)_\rho / (\partial E/\partial T)_\rho$ . HYADES determined the sound speed using Eq. (14), where the thermodynamic derivatives were found from the equations of state (EOS) from the SESAME library (Los Alamos National Laboratory, USA). We used the SESAME EOS 5171 (HYADES EOS 93) for argon and SESAME EOS 7153 (HYADES EOS 315) for water.

Figure 1 shows the bubble radius  $R(t)$ , the bubble-wall velocity  $U(t) = dR/dt$ , the sound speed in the liquid at the bubble wall  $C(t)$ , and the bubble-wall Mach number  $U/C$ . At the moment of the collapse ( $t = 0$ , dashed line) the bubble-wall implosion came to an end, bringing the bubble to its minimum radius [Fig. 1(a)]. The bubble-wall velocity  $U$  [Fig. 1(b)] was negative during the implosion ( $t < 0$ ) and positive during the rebound phase. Here we consider only the implosion phase.

During the last  $\sim 10.7$  ns prior to the moment of the collapse, the sound speed in the liquid at the bubble wall  $C$  was rapidly increasing [Fig. 1(c)]. This increase of  $C$  was faster than the increase of  $|U|$ , so that the magnitude of the bubble-wall Mach number  $U/C$  [Fig. 1(d)] started to decrease even though  $|U|$  continued to increase until  $t \approx -3.5$  ns [Fig. 1(b)]. As a consequence, the bubble-wall Mach number  $U/C$  reached its maximum magnitude of  $\sim 1.4$  at  $t \approx -10.7$  ns [Fig. 1(d)].

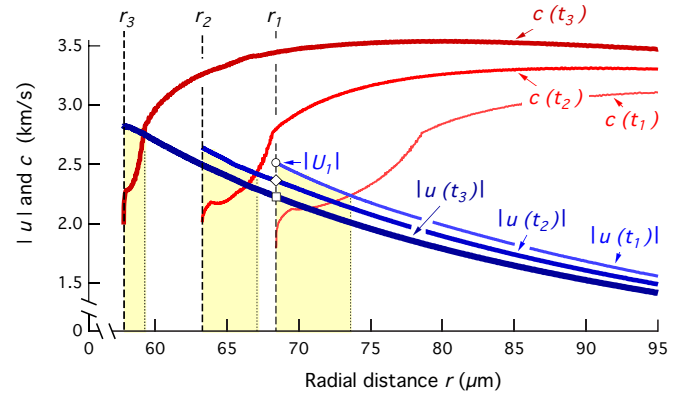


FIG. 2. Velocity magnitude  $|u|$  and sound speed  $c$  in the liquid at three moments in time:  $t_1 = -14.7$  ns,  $t_2 = -12.7$  ns, and  $t_3 = -10.7$  ns. Bubble-wall positions are shown by the dashed lines:  $r_1 = 68.5$   $\mu\text{m}$  at  $t_1$ ,  $r_2 = 63.3$   $\mu\text{m}$  at  $t_2$ , and  $r_3 = 57.8$   $\mu\text{m}$  at  $t_3$ . Bubble's interior (to the left of the dashed lines) is not shown. Dotted lines mark the locations of  $|u| = c$ :  $73.7$   $\mu\text{m}$  at  $t_1$ ,  $67$   $\mu\text{m}$  at  $t_2$ , and  $59.2$   $\mu\text{m}$  at  $t_3$ . The highlights (between the dashed and the dotted lines) indicate regions with supersonic velocities.

Figure 2 shows radial distributions of liquid velocity magnitude  $|u|$  and sound speed  $c$  in the liquid around the imploding bubble at three moments in time. The bubble wall was moving toward the bubble center (from right to left in Fig. 2) with supersonic velocities:  $U_1 = 2516$  m/s at  $t_1$ ,  $U_2 = 2640$  m/s at  $t_2$ , and  $U_3 = 2827$  m/s at  $t_3$ . The velocity of the liquid proximal to the bubble (highlighted regions) was also supersonic. To the right of the dotted lines, the liquid velocity was subsonic due to a decrease of  $|u|$  and an increase of  $c$  in the proximity to the bubble.

Figure 2 can be used to assess  $u \partial u/\partial r$  and  $\partial u/\partial t$ . The derivative  $\partial u/\partial r$  is given by the slope of  $u(r)$  at a fixed moment in time, while  $\partial u/\partial t$  is a change of velocity  $u$  at a fixed distance  $r$ . Let us estimate these terms at  $r_1$ . In the  $\pm 2$  ns time interval around  $t_2$ , the velocity magnitude changed from  $u_1(r_1) = 2516$  m/s (circle) to  $u_3(r_1) = 2226$  m/s (square). Dividing this change by 4 ns gives  $\partial u/\partial t$  as  $7.3\text{E} + 10$  m/s<sup>2</sup>. To estimate  $u \partial u/\partial r$ , we multiply the liquid velocity  $u_2$  at  $r_1$  (2360 m/s, diamond) by the slope of the curve  $u_2$  at  $r_1$  ( $4.2\text{E} + 7\text{s}^{-1}$ ). This gives  $u \partial u/\partial r \approx -9.9\text{E} + 10$  m/s<sup>2</sup>, showing that the convective term  $u \partial u/\partial r$  and the partial time derivative  $\partial u/\partial t$  had the same orders of magnitude.

The derivatives  $\partial u/\partial t$  and  $u \partial u/\partial r$  had opposing signs. The sum of these two terms gives the material time derivative  $du/dt = \partial u/\partial t + u \partial u/\partial r$ , i.e., the acceleration of a liquid particle as it moves in space. The acceleration of the bubble wall  $dU/dt$  is the slope of the curve  $U(t)$  in Fig. 1(b). When the slope was negative, the bubble wall was accelerating toward the bubble center, and the magnitude of  $u \partial u/\partial r$  exceeded  $\partial u/\partial t$ . These two terms became equal in magnitude at  $t \approx -3.5$  ns, when the slope of  $U(t)$  was zero ( $dU/dt = 0$ ) and the bubble-wall velocity reached its greatest magnitude of 3.84 km/s [Fig. 1(b)]. After that, the bubble-wall velocity decelerated [ $dU/dt > 0$ , Fig. 1(b)]. During the final 1.2 ns of the implosion, both  $\partial u/\partial t$  and  $u \partial u/\partial r$  were positive. Their sum  $dU/dt$  reached a broad maximum of  $3.4\text{E} + 12$  m/s<sup>2</sup> at  $\sim 0.4$  ns prior to the moment of the collapse.

Let us now consider a steady flow in a converging tube, as it is instructive to discuss a known example when the fundamental theory of fluid dynamics limits velocities by the sound speed (Ref. [3], §97). For the steady adiabatic flow we can use Eq. (7) (Eq. (A1) in Ref. [4])

$$\frac{d\rho}{du} = -\rho \frac{u}{c^2}. \quad (15)$$

Multiplying it by  $u$  and substituting  $u d\rho$  from the identity  $u d\rho = d(u\rho) - \rho du$  gives a relation (Eq. 83.5 in Ref. [3])

$$\frac{d(u\rho)}{du} = \rho \left(1 - \frac{u^2}{c^2}\right). \quad (16)$$

This relation is valid along streamlines and shows that the magnitude of the mass flux density  $j \equiv u\rho$  behaves differently for subsonic and supersonic velocities. For subsonic velocities ( $|u| < c$ ), an increase of velocity magnitude  $|u|$  increases  $j$ . For supersonic velocities ( $|u| > c$ ), an increase of  $|u|$  decreases  $j$ . The mass flux density reaches maximum at  $|u| = c$  and vanishes along with the density  $\rho$  at some maximum velocity ( $|u_{\max}| > c$ ), attained by the flow out into a vacuum (Ref. [3]).

One can use Eq. (16) to show that it is impossible to reach supersonic velocities in a steady flow through a continually narrowing tube [3]. Let us assume that the flow at the inlet of the tube is subsonic, and that the cross section of the tube is relatively small and slowly narrowing such that the mass flux density  $\mathbf{j}$  is parallel to the axis of symmetry in every cross section. For a time-independent flow, the mass passing through every cross section in unit time is the same so that a decrease of the cross-sectional area is associated with an increase of the mass flux per unit area,  $j$ . As the right-hand side of Eq. (16) for the subsonic velocities is positive, the increase of  $j$  requires an increase of  $u$ . Thus, the velocity  $u$  increases along the converging tube. The increasing velocity  $u$ , however, cannot become supersonic, as the right-hand side of Eq. (16) would become negative, decreasing  $j$ , which contradicts the increase of  $j$  along the converging tube. The steady-flow velocity can reach the sound speed only at the outlet of the converging tube and become supersonic in a diverging tube [3].

For the unsteady flow, the above argumentation is inapplicable. First, we cannot invoke the requirement that the mass flux must be the same through every cross section, as the mass may vary in time. For example, the mass in a given region may increase at one moment in time and decrease at a later moment in time. Second, Eq. (16) was derived neglecting the partial time derivative  $\partial u/\partial t$ , i.e., assuming that the flow was in the steady state.

The inapplicability of Eq. (16) for the unsteady flow around the collapsing bubbles is illustrated in Fig. 3, showing the mass flux density in the liquid around the imploding bubble at a fixed moment in time. In the region with supersonic velocities (highlighted), the velocity magnitude  $|u|$  increases monotonically toward the bubble wall (from right to left), but the mass flux density is nonmonotonic, reaching the maximum at  $r \approx 70 \mu\text{m}$ . This differs from the steady flow, for which—according to Eq. (16)—the mass flux density would monotonically increase with  $r$  in the highlighted region with supersonic velocities (from the bubble wall to the vertical

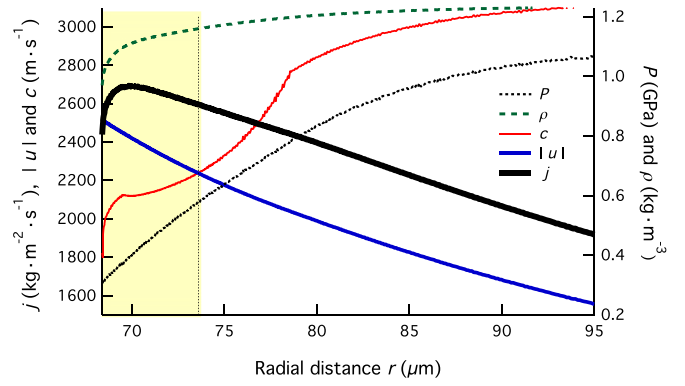


FIG. 3. Mass flux density  $j$ , velocity magnitude  $|u|$ , sound speed  $c$ , pressure  $P$ , and density  $\rho$  in the liquid near the bubble wall (left-most position) at  $t = -14.7$  ns. The supersonic region (highlighted) extends from the bubble wall to  $r = 73.7 \mu\text{m}$  (vertical dotted line).

dotted line at  $r \approx 73.7 \mu\text{m}$ ) and decrease with  $r$  in the region with subsonic velocities ( $r > 73.7 \mu\text{m}$ ).

Figure 3 also shows the pressure, the density, and the sound speed in the liquid around the collapsing bubble. The sound speed increased with the pressure, reaching approximately 3000 m/s at pressure of 1 GPa.

The dependence of sound speed on pressure in water can be illustrated using the isentropic equation of Tait

$$\frac{P + B}{P_0 + B} = \left(\frac{\rho}{\rho_0}\right)^n, \quad (17)$$

where  $B$  and  $n$  are fitting parameters, and  $\rho_0$  is the density at the reference pressure  $P_0$ . Figure 4 shows the sound speed  $c = \sqrt{dP/d\rho}$  calculated using  $P_0 = 0.1$  MPa,  $\rho_0 = 997 \text{ kg/m}^3$ , and three sets of fitting parameters  $B$  and  $n$  from previous studies [34–36].

The increase of the sound speed with pressure (Fig. 4) is among the main factors reducing the extent of the supersonic region around the collapsing bubbles. The dependence of the sound speed on pressure (Fig. 4) also shows the need to know the pressure (or density) to determine whether the bubble-wall velocity is supersonic. For example, recent experiments at high static pressure have shown bubble-wall velocities as high as

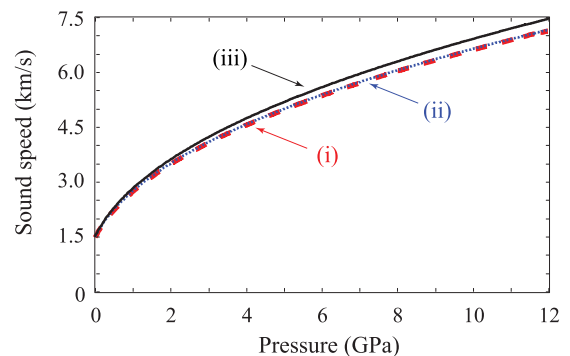


FIG. 4. Sound speed vs pressure calculated using Eq. (17) with three sets of parameters: (i)  $B = 300$  MPa and  $n = 7$  (red dashed line, Ref. [34]), (ii)  $B = 314$  MPa and  $n = 7$  (dotted blue, Ref. [35]), and (iii)  $B = 295.5$  MPa and  $n = 7.44$  (solid black, Ref. [36]).

7.5 km/s [27]. According to Fig. 4, these bubble-wall velocities would remain supersonic up to the pressure of 12 GPa.

In conclusion, the present analysis shows that the upper bound on the bubble-wall velocity [4] appears to be derived omitting the partial derivatives with respect to time. This steady-flow assumption requires justification, as the partial time derivatives can have the same orders of magnitude as the other terms in the hydrodynamic equations. Furthermore, the results of numerical simulations from this (Figs. 1–3) and other studies [29–31,33] show bubble-wall velocities greater

than the sound speed in the liquid at the bubble wall. This poses a question on the extent to which the upper bound is applicable for the collapsing bubbles.

The author thanks S. E. Nicholson for HYADES simulations and the development of HYADES visualization software, as well as for proofreading this manuscript, Dr. J. T. Larsen for advice on the HYADES code, and Dr. D. F. Gaitan for his contribution to adapt the HYADES code for modeling cavitation bubbles.

- 
- [1] W. Besant, *A treatise on hydrostatics and hydrodynamics* (Deighton, Bell, Cambridge, 1859).
- [2] L. Rayleigh, *Philos. Mag. Ser. 6* **34**, 94 (1917).
- [3] L. Landau and E. Lifschitz, *Fluid mechanics*, 2nd ed. (Pergamon Press, Oxford, 1987), pp. 1–539.
- [4] K. Yasui, *Phys. Rev. E* **64**, 016310 (2001).
- [5] D. F. Gaitan, in *Proc. Int. Symp. Sustain. Acoust. ISSA 2010* (Auckland, 2010), pp. 1–7.
- [6] W. C. Moss, D. B. Clarke, J. W. White, and D. A. Young, *Phys. Lett. Sect. A* **211**, 69 (1996).
- [7] R. P. Taleyarkhan, C. D. West, J. S. Cho, R. T. Lahey Jr., R. I. Nigmatulin, and R. C. Block, *Science* **295**, 1868 (2002).
- [8] R. P. Taleyarkhan, J. S. Cho, C. D. West, R. T. Lahey, R. I. Nigmatulin, and R. C. Block, *Phys. Rev. E* **69**, 036109 (2004).
- [9] C. G. Camara, S. D. Hopkins, K. S. Suslick, and S. J. Putterman, *Phys. Rev. Lett.* **98**, 064301 (2007).
- [10] D. F. Gaitan and R. Tessien, *J. Acoust. Soc. Am.* **113**, 2206 (2003).
- [11] D. F. Gaitan, R. A. Tessien, R. A. Hiller, and J. Alstadter, *J. Acoust. Soc. Am.* **122**, 2991 (2007).
- [12] D. F. Gaitan and R. A. Hiller, *J. Acoust. Soc. Am.* **123**, 3559 (2008).
- [13] D. F. Gaitan, R. A. Tessien, R. A. Hiller, J. Gutierrez, C. Scott, H. Tardif, B. Callahan, T. J. Matula, L. A. Crum, R. G. Holt, C. C. Church, and J. L. Raymond, *J. Acoust. Soc. Am.* **127**, 3456 (2010).
- [14] D. F. Gaitan, Y. A. Pishchalnikov, T. J. Matula, C. C. Church, J. Gutierrez, C. Scott, R. G. Holt, and L. A. Crum, *J. Acoust. Soc. Am.* **129**, 2619 (2011).
- [15] C. C. Church, D. F. Gaitan, Y. A. Pishchalnikov, and T. J. Matula, *J. Acoust. Soc. Am.* **129**, 2620 (2011).
- [16] T. Matula, B. MacConnaghy, L. Crum, and F. Gaitan, *J. Acoust. Soc. Am.* **129**, 2619 (2011).
- [17] P. Anderson, A. Sampathkumar, and R. G. Holt, *J. Acoust. Soc. Am.* **129**, 2620 (2011).
- [18] D. F. Gaitan, J. Gutierrez, Y. A. Pishchalnikov, M. Coffin, and H. Tardif, *J. Acoust. Soc. Am.* **129**, 2620 (2011).
- [19] R. G. Holt, P. A. Anderson, A. Sampathkumar, J. R. Sukovich, and D. F. Gaitan, *J. Acoust. Soc. Am.* **129**, 2619 (2011).
- [20] J. B. Lonzaga, J. L. Raymond, J. Mobley, and D. F. Gaitan, *J. Acoust. Soc. Am.* **129**, 597 (2011).
- [21] Y. A. Pishchalnikov, D. F. Gaitan, M. S. Einert, R. G. Holt, C. C. Church, and L. A. Crum, *J. Acoust. Soc. Am.* **129**, 2620 (2011).
- [22] P. Anderson, A. Sampathkumar, T. W. Murray, D. F. Gaitan, and R. G. Holt, *J. Acoust. Soc. Am.* **130**, 3389 (2011).
- [23] K. B. Bader, J. Mobley, C. C. Church, and D. F. Gaitan, *J. Acoust. Soc. Am.* **132**, 2286 (2012).
- [24] K. B. Bader, J. L. Raymond, J. Mobley, C. C. Church, and D. Felipe Gaitan, *J. Acoust. Soc. Am.* **132**, 728 (2012).
- [25] J. R. Sukovich, A. Sampathkumar, P. A. Anderson, R. G. Holt, Y. A. Pishchalnikov, and D. F. Gaitan, *Phys. Rev. E* **85**, 056605 (2012).
- [26] Y. A. Pishchalnikov, J. Gutierrez, W. W. Dunbar, and R. W. Philpott, *Ultrasonics* **65**, 380 (2016).
- [27] J. R. Sukovich, P. A. Anderson, A. Sampathkumar, D. F. Gaitan, Y. A. Pishchalnikov, and R. G. Holt, *Phys. Rev. E* **95**, 043101 (2017).
- [28] K. Yasui, *J. Chem. Phys.* **115**, 2893 (2001).
- [29] F. R. Gilmore, Calif. Inst. Technol. Rept. **26**, 1 (1952).
- [30] R. Hickling and M. S. Plesset, *Phys. Fluids* **7**, 7 (1964).
- [31] V. A. Akulichev, in *High-Intensity Ultrasonic Fields*, edited by L. D. Rozenberg (Plenum Press, New York, 1971).
- [32] J. T. Larsen and S. M. Lane, *J. Quant. Spectrosc. Radiat. Transfer* **51**, 179 (1994).
- [33] W. C. Moss, D. B. Clarke, J. W. White, and D. A. Young, *Phys. Fluids* **6**, 2979 (1994).
- [34] R. Hickling, *Phys. Rev. Lett.* **73**, 2853 (1994).
- [35] A. Vogel, S. Busch, and U. Parlitz, *J. Acoust. Soc. Am.* **100**, 148 (1996).
- [36] J. Staudenraus and W. Eisenmenger, *Ultrasonics* **31**, 267 (1993).